Figures

Note that all figures are scaled by a factor of 2 for display.

Figure 1: Location of the ice camp located near the Qikiqtarjuaq Island in the Baffin Bay. Projection used: EPSG-4326.

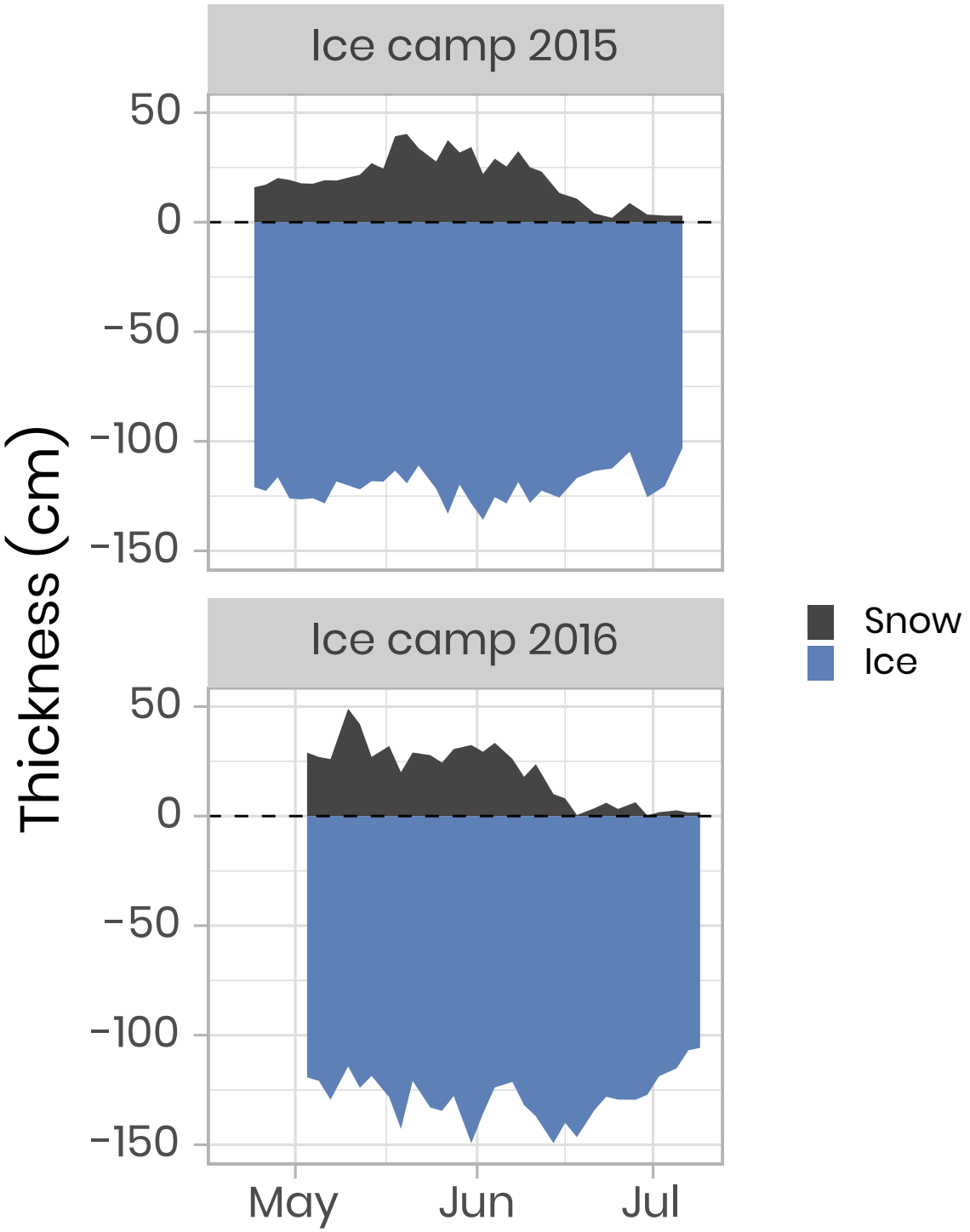

Figure 2: Temporal evolution of the snow and sea-ice thickness for both ice camp missions. The dashed horizontal line represents the snow/ice interface.

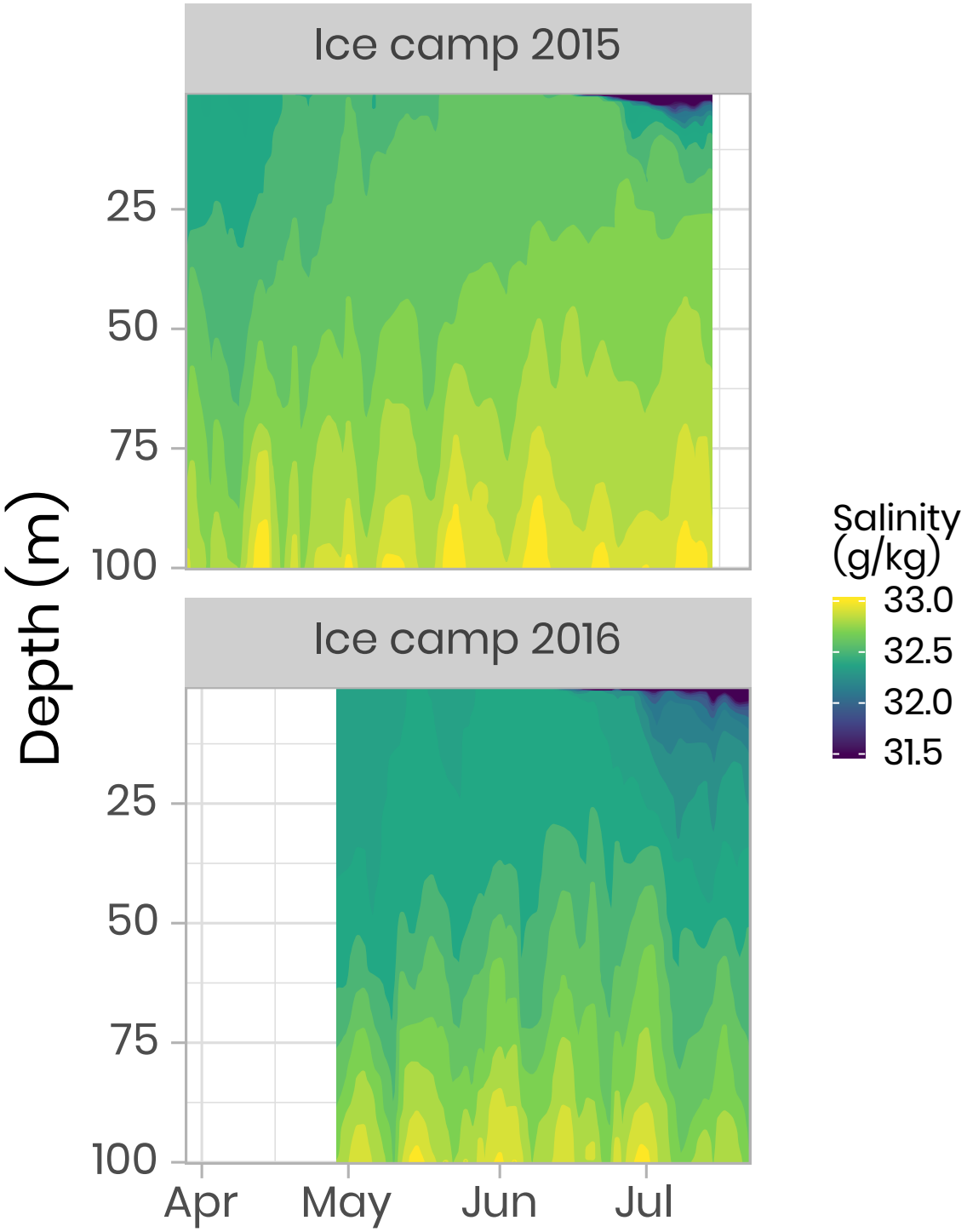

Figure 3: Temporal evolution of the salinity in the first 100 meters of the water column for both campaigns. Note that for visualization, salinity below 31.5 g kg^{-1} have been binned to 31.5 g kg^{-1}.

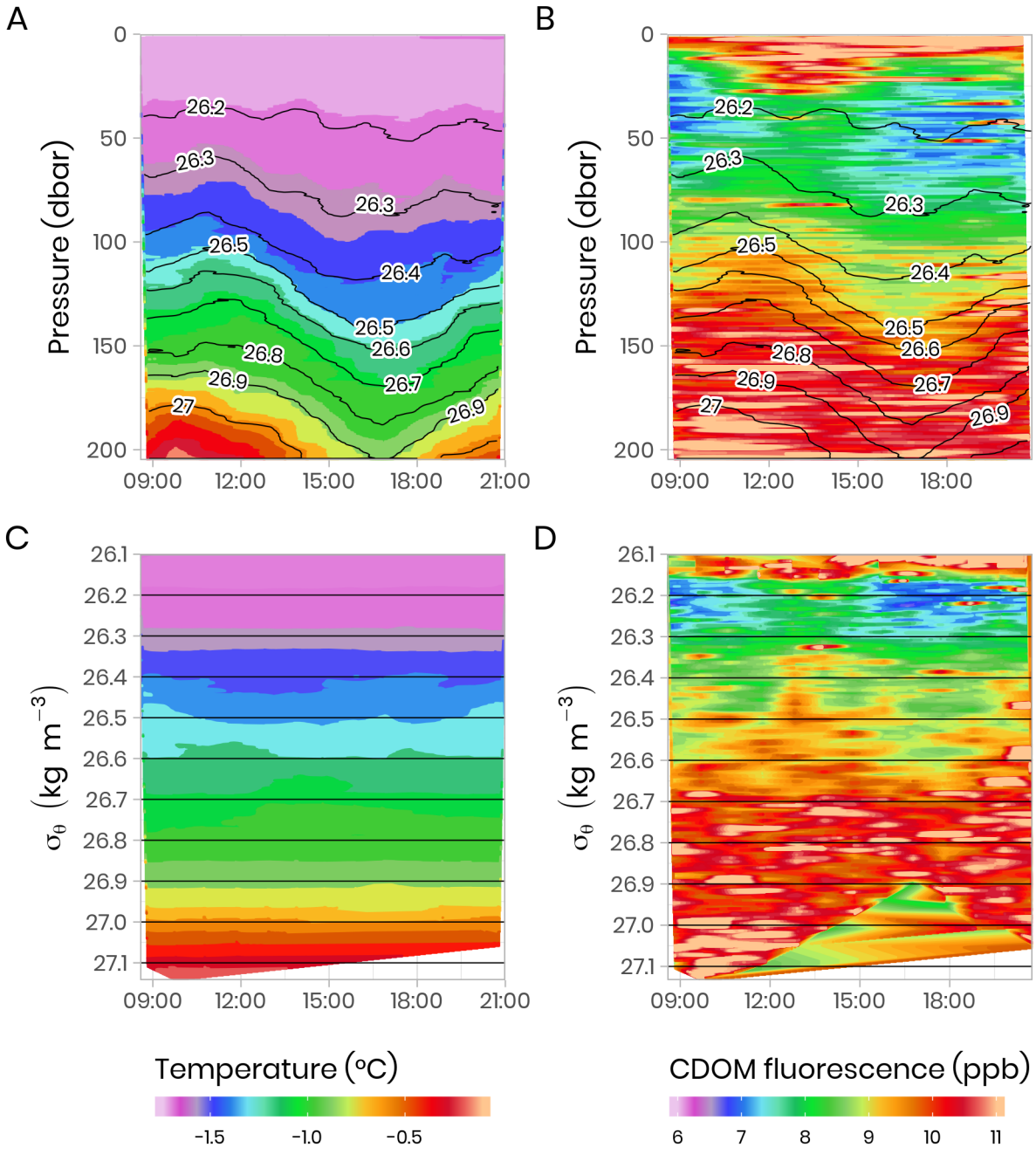

Figure 4: Temporal evolution of physical (temperature) and bio-optical (CDOM fluorescence) variables with superimposed lines of potential density anomaly (σ_θ, kg m^{-3}) during a 13-h tidal cycle. Surface tidal height versus time at Qikiqtarjuaq is shown in blue. (A-B) Plotted versus pressure coordinates (equivalent to depth in meters). (C-D) The same data plotted versus potential density anomaly σ_θ coordinates (kg m^{-3}). The tidal survey was performed on 2015-06-09.

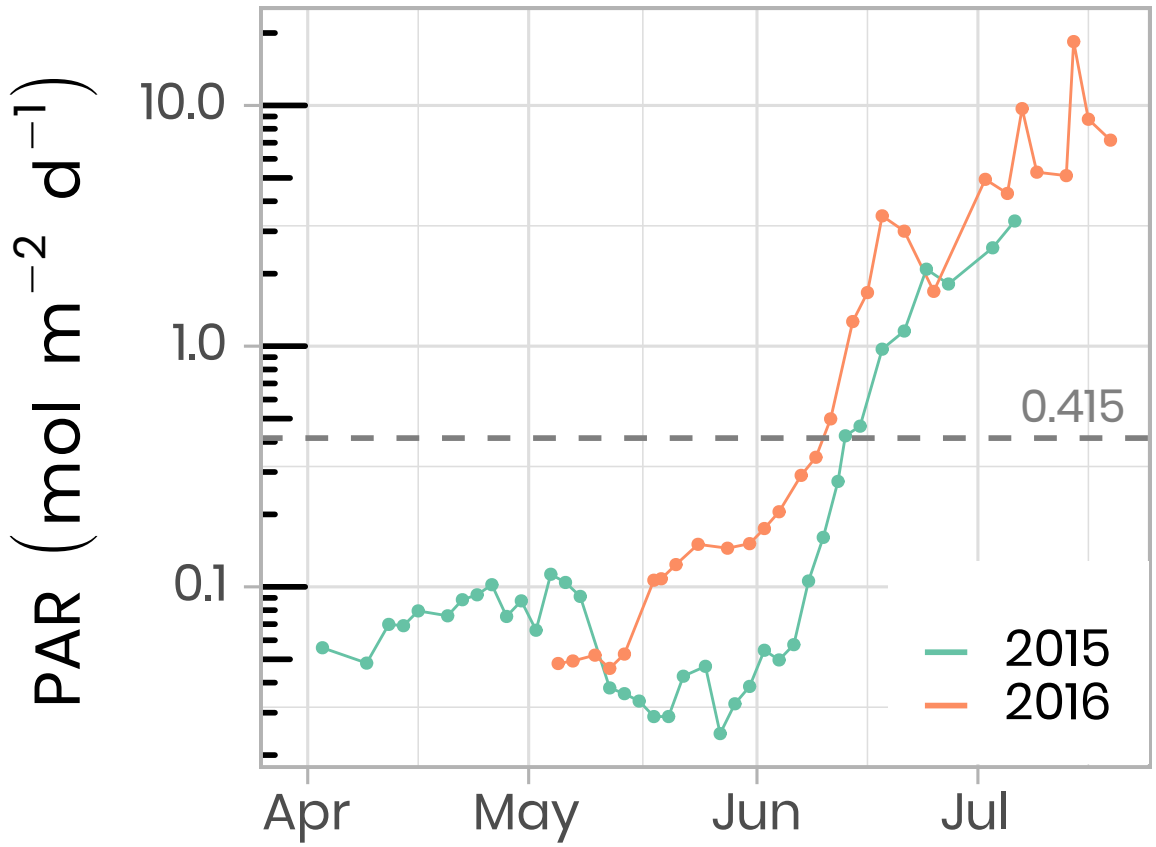

Figure 5: Temporal evolution of daily photosynthetically available radiation (PAR) at the sea-ice/water interface (1.3 m depth) for both ice camp missions. The horizontal dashed line shows the 0.415 mol photons m^{-2} d^{-1} threshold often used in the literature as the minimum light requirement for primary production.

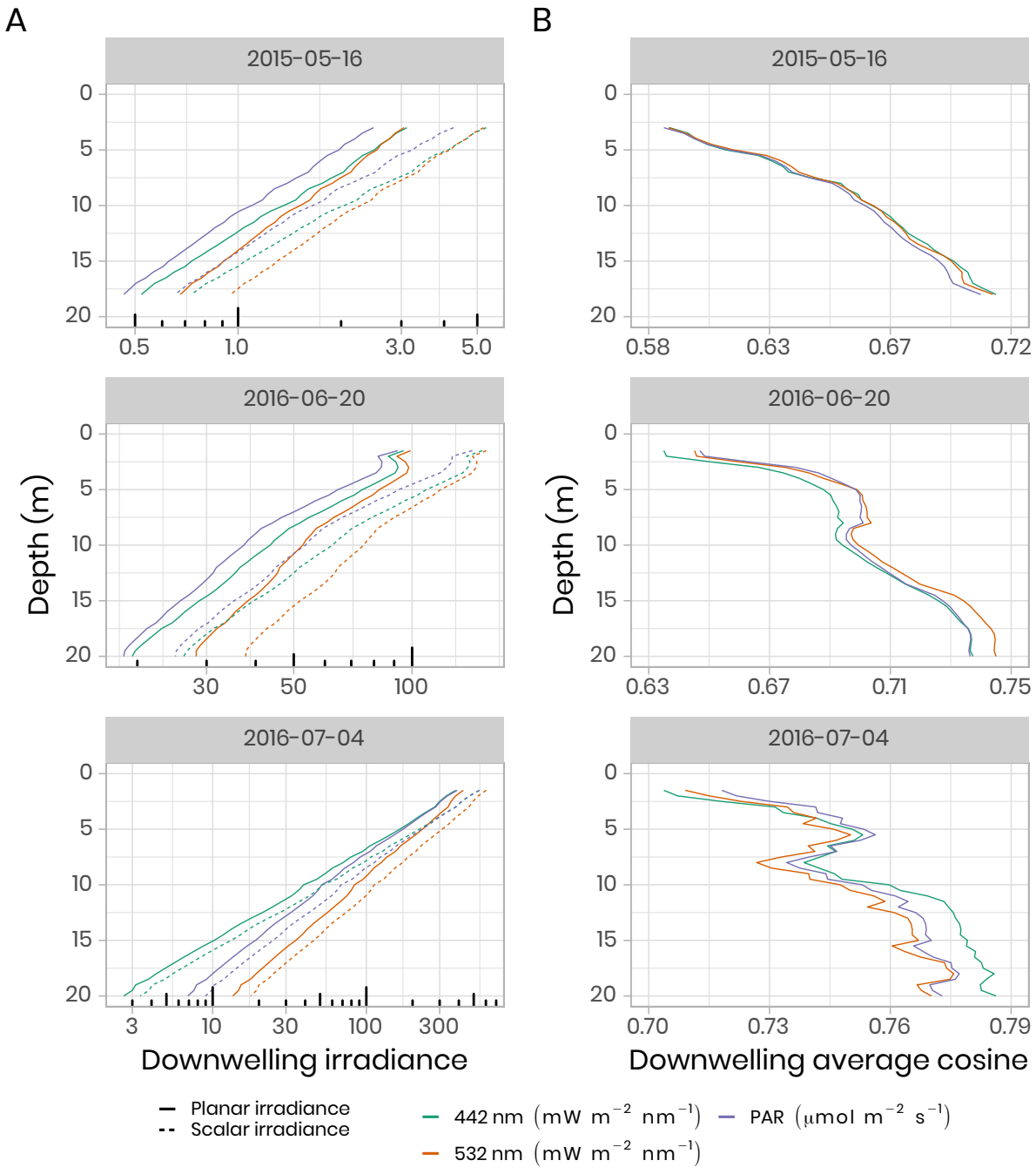

Figure 6: (A) Under-ice vertical profiles of downwelling planar and scalar irradiance at 442 nm, 532 nm and for PAR. (B) Calculated downwelling average cosine (unitless) was measured beneath snow-covered sea ice on 16 May 2015, beneath bare ice on 20 June 2016 and beneath a melt pond on 4 July 2016. Note the log scale for the irradiance measurements (A).

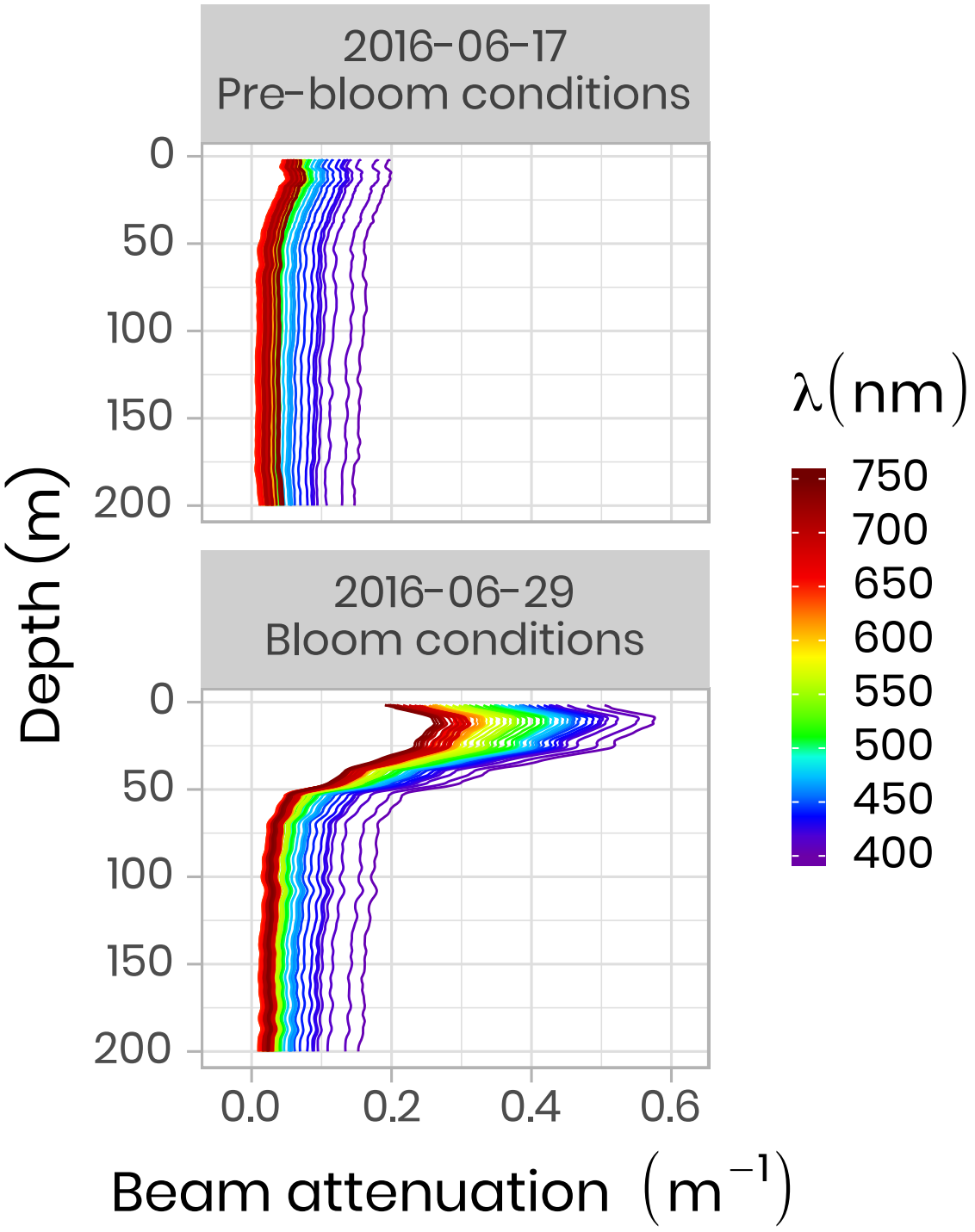

Figure 7: Beam attenuation coefficients (c, m^{-1}) measured in 2016 using an ACS before and during the phytoplankton bloom. Note that the colors of the lines correspond to wavelength frequencies.

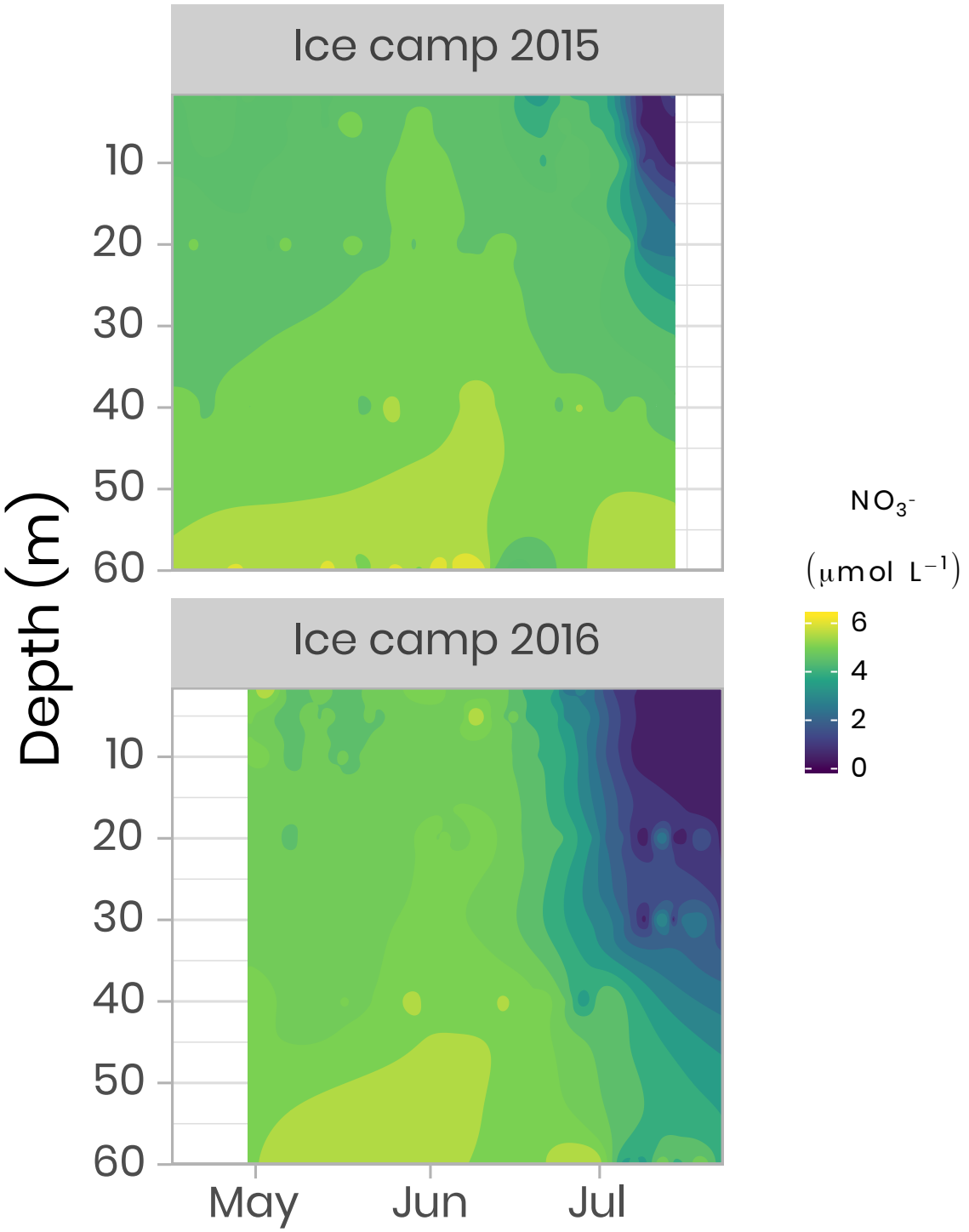

Figure 8: Temporal evolution of the nitrates in the first 60 m of the water column for both ice camp missions.

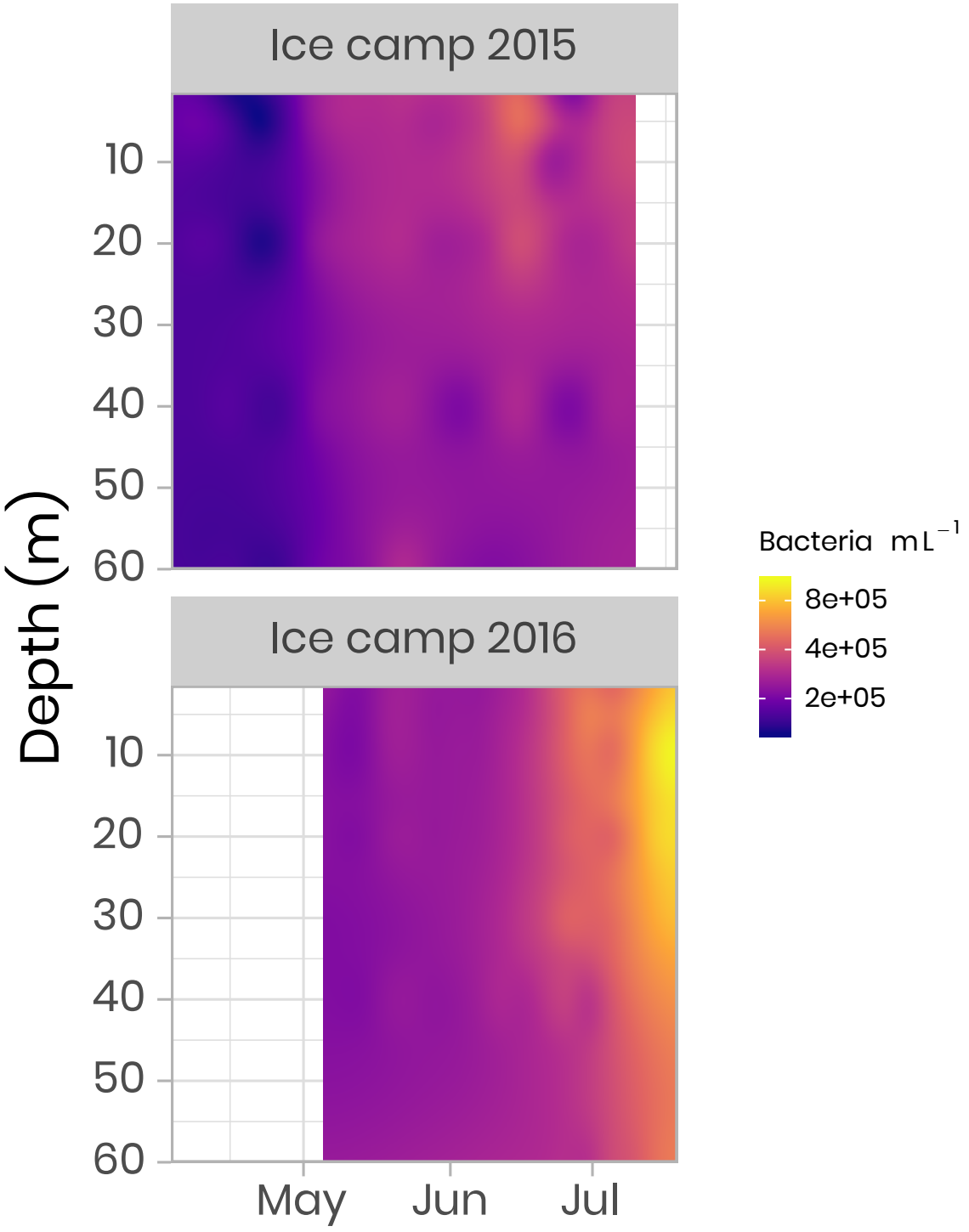

Figure 9: Concentration of bacteria in the water column at the ice camp in 2015 and 2016.

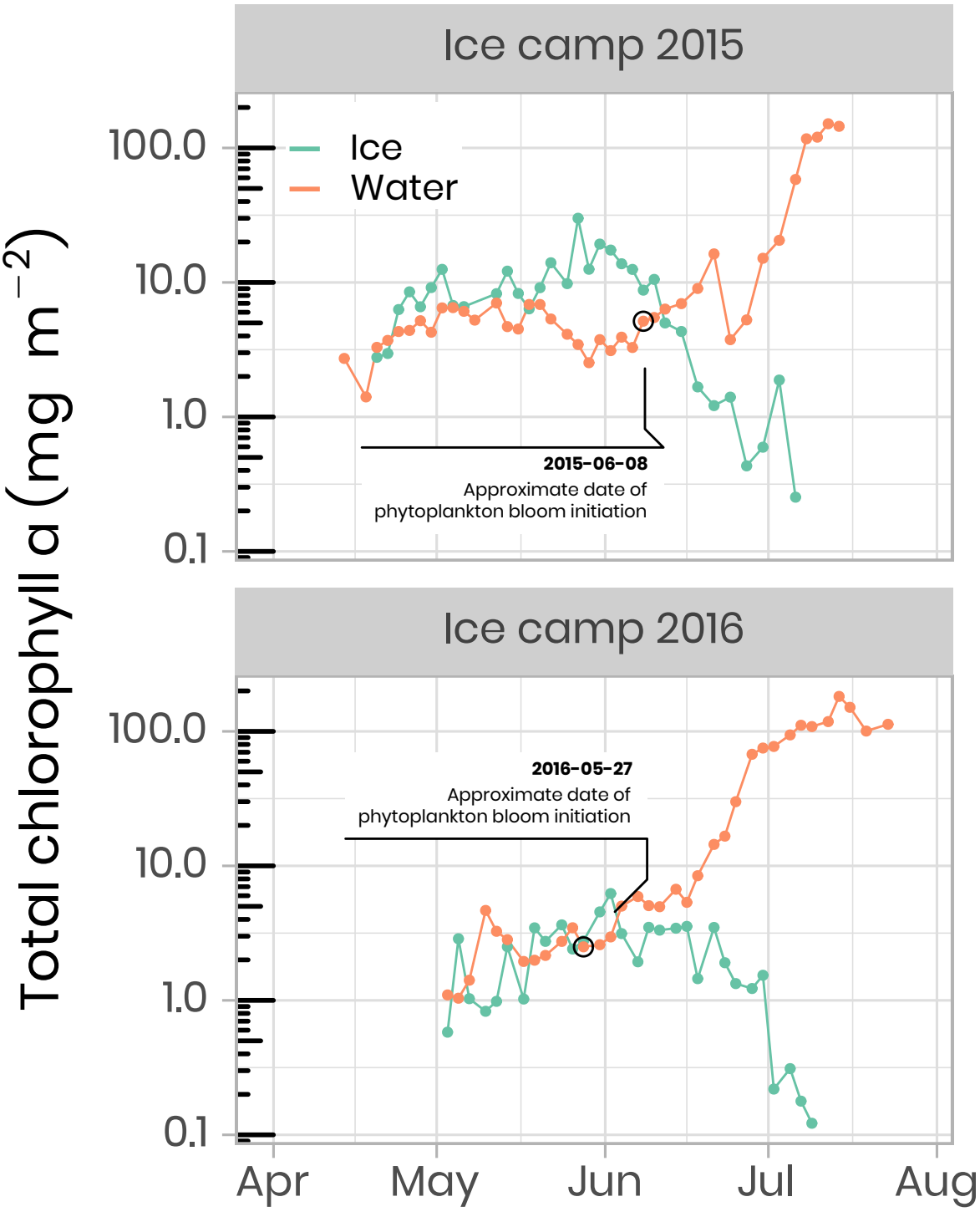

Figure 10: Temporal evolution of chlorophyll a in ice and water (depth-integrated) for both ice camp missions. Note that the water chlorophyll a have been integrated over the first 100 m of the water column whereas the ice chlorophyll a was measured on the bottom 0-10 cm of the ice cores. The details of the calculations to determine the approximate dates of phytoplankton bloom initiation can be found in Oziel et al. (2019).

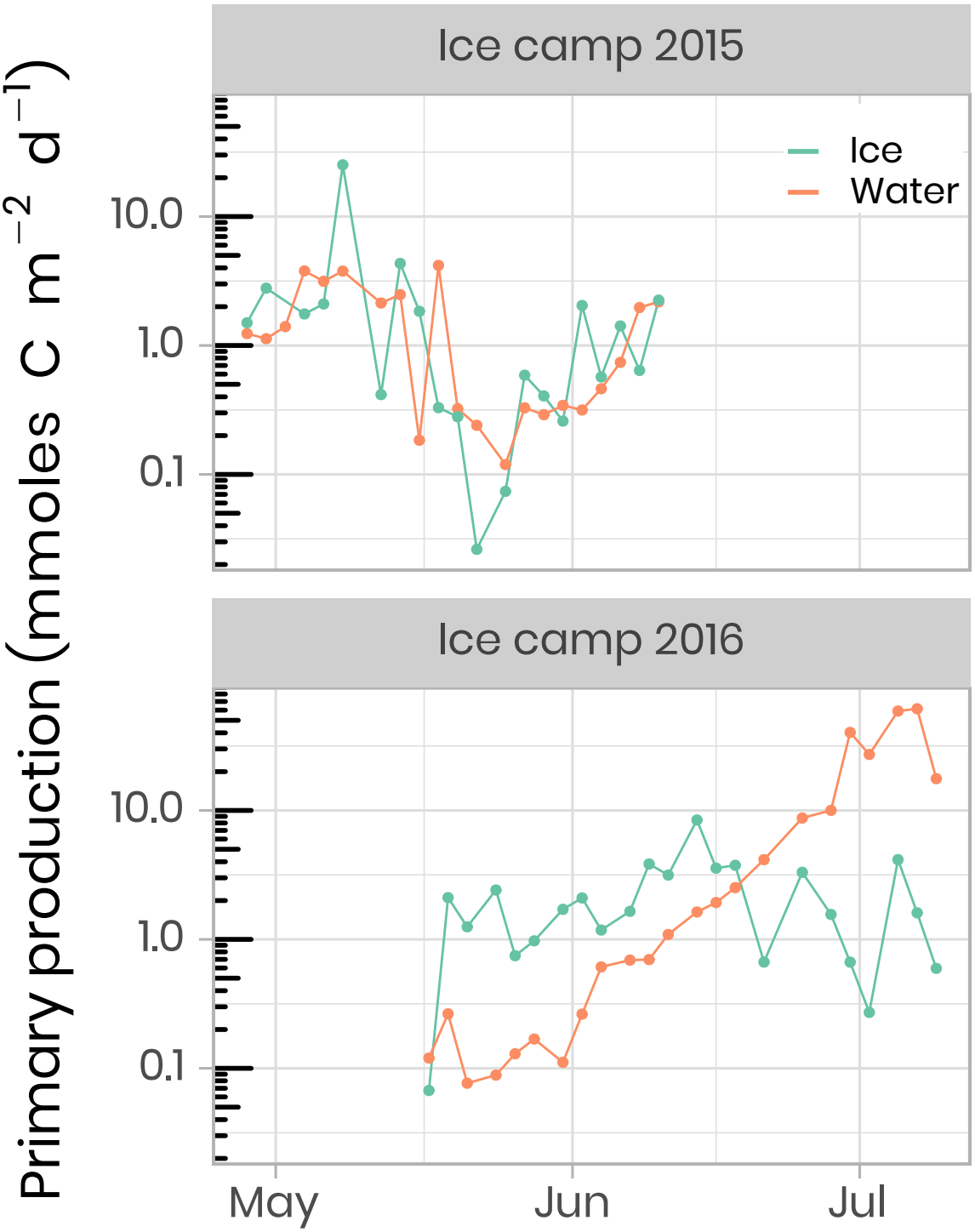

Figure 11: Temporal evolution of primary production a in ice and water (depth-integrated) for both ice camp missions.

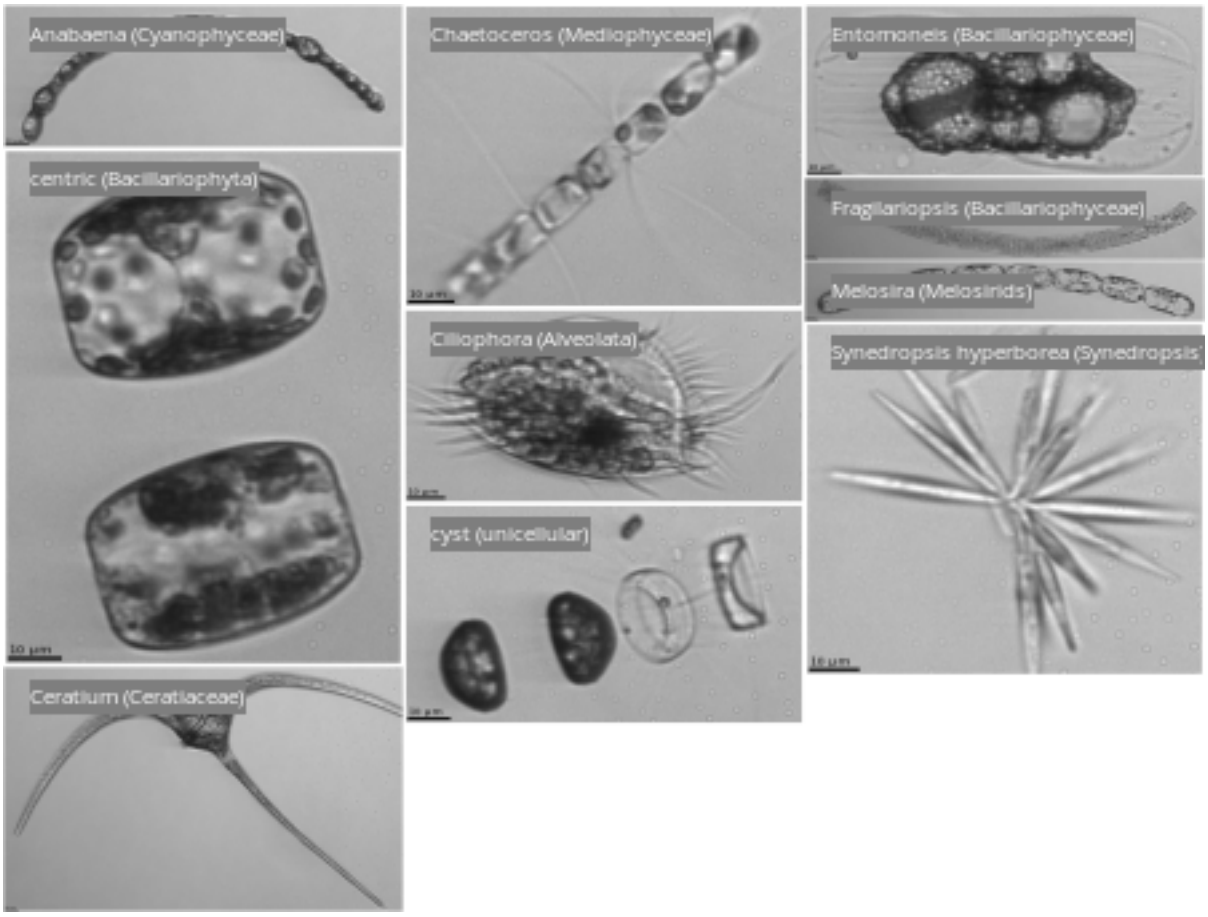

Figure 12: Taxo. TODO: I asked P.-L. to produce a better composite image.

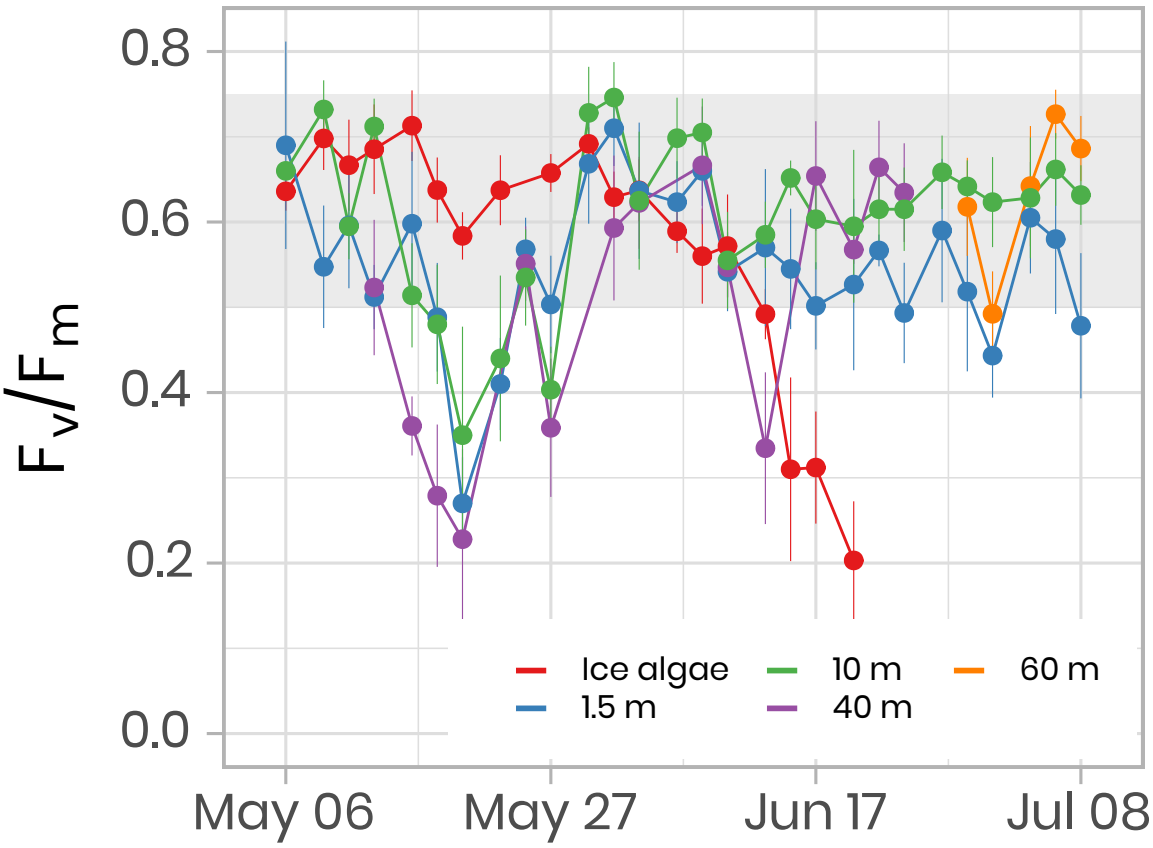

Figure 13: Temporal evolution of F_v/F_m for ice (last cm) and water underneath the ice (depths 1.5 m, 10 m, 40 m) samples for the ice camp 2016 between May 6th and July 8th. F_v/F_m monitoring on ice samples stopped on Day 172-June 20th because the Chl a fluorescence signal was not reliable anymore. F_v/F_m monitoring on 40 m and 60 m depth samples was limited between May 13th and June 24th and between June 29th-July 08th, respectively. The gray shaded area represents the range at which the algae are optimally growing.

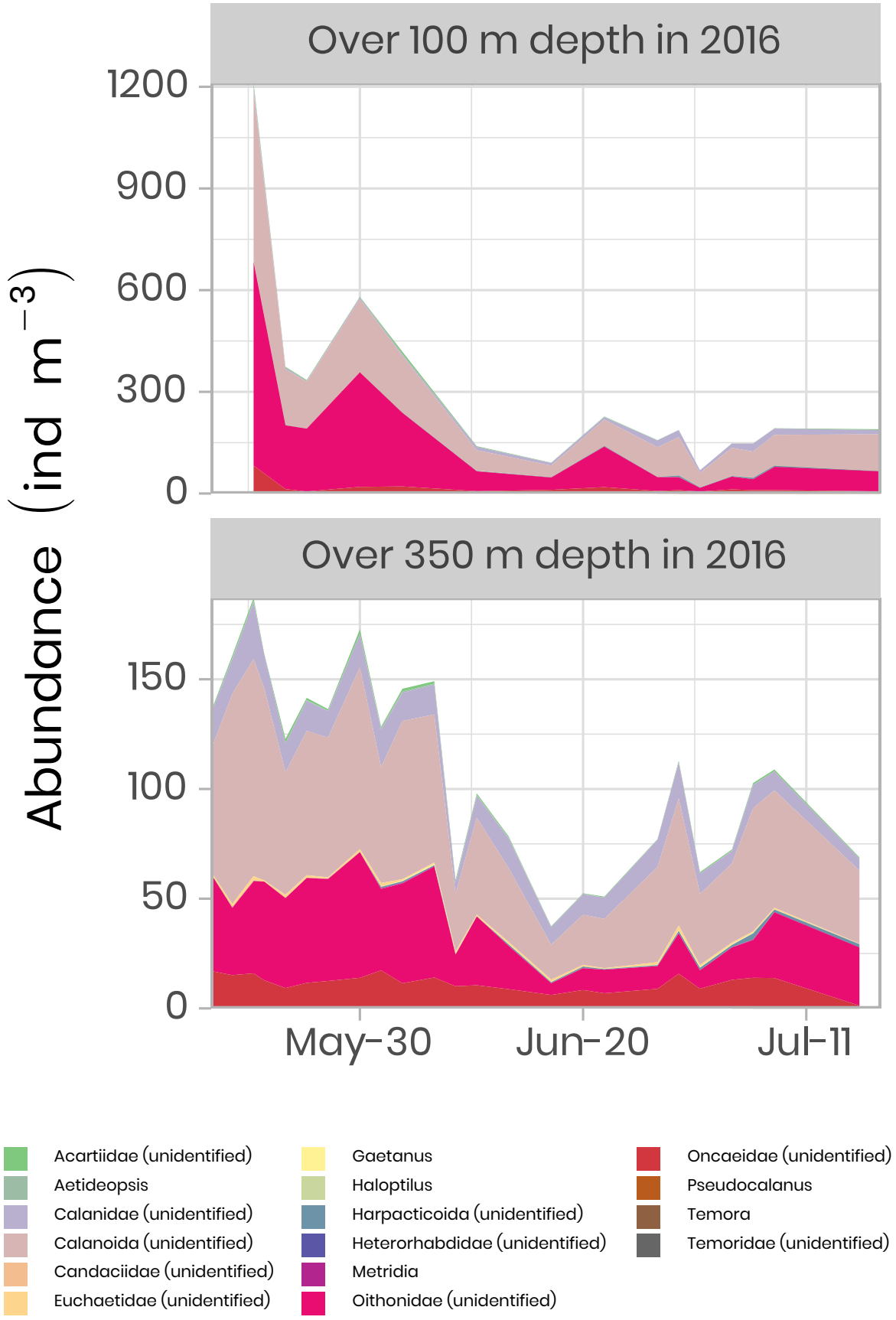

Figure 14: Time series of the abundance of the copepoda (ind m^{-1}) measured over the first 100 m and 350 m of the water column in 2016 using the zooscan.